

Bottomonium on a lattice

orbital excitations and radiative transitions

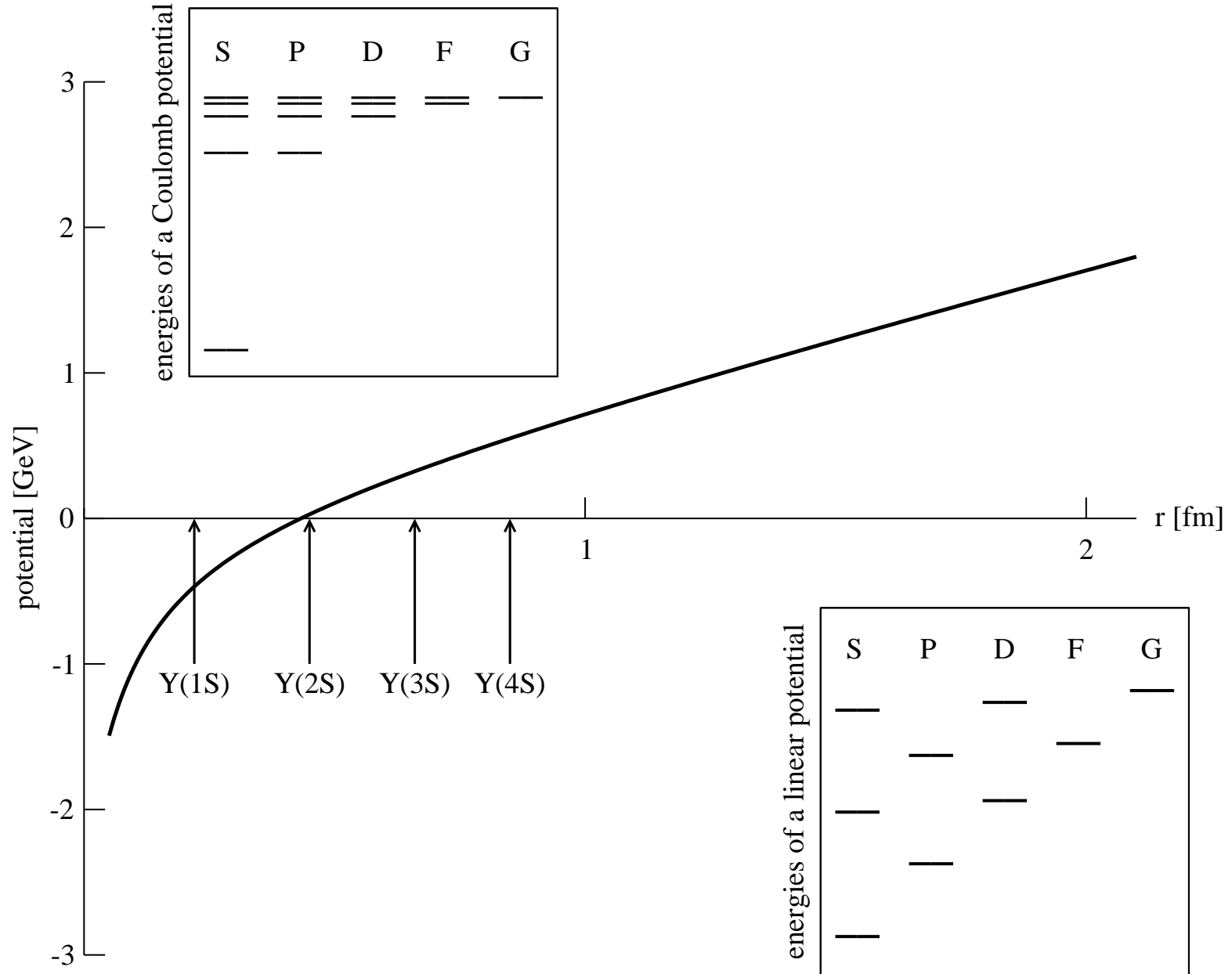
- masses of S, P, D, F and G waves
- M1 transitions among S waves

R. Lewis and R. M. Woloshyn, Phys. Rev. D84, 094501 (2011).

R. Lewis and R. M. Woloshyn, Phys. Rev. D85, 114509 (2012).

R. Lewis and R. M. Woloshyn, Phys. Rev. D86, 057501 (2012).

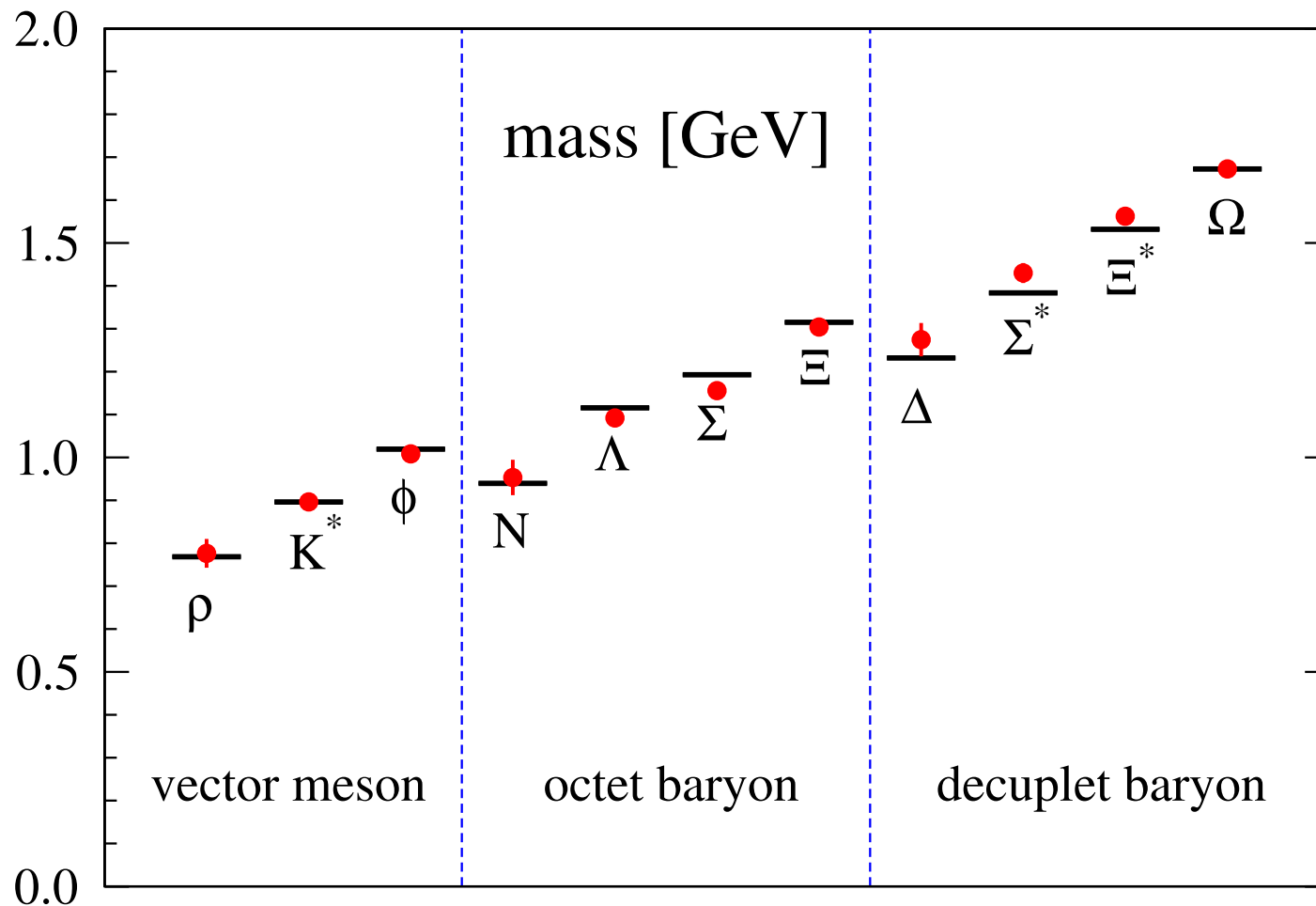
Coulomb and linear potentials



The PACS-CS configurations

S. Aoki *et al.* Phys. Rev. D79, 034503 (2009).

- Iwasaki+clover improved action. We use one ensemble of 198 configurations.
- $m_u=m_d \gtrsim$ physical ($m_\pi=156$ MeV) and $m_s \gtrsim$ physical ($m_K=553$ MeV).
- $32^3 \times 64$ lattices with $\beta = 1.90 \Rightarrow a=0.0907(14)$ fm and $L = 32a = 2.9$ fm.
- Parameters are set using m_π , m_K and m_Ω as input.



Tadpole-improved NRQCD action

$$\begin{aligned} H = & \frac{-\Delta^{(2)}}{2M_0} - c_1 \frac{(\Delta^{(2)})^2}{8M_0^3} + \frac{c_2}{U_0^4} \frac{ig}{8M_0^2} (\Delta \cdot \mathbf{E} - \mathbf{E} \cdot \Delta) \\ & - \frac{c_3}{U_0^4} \frac{g}{8M_0^2} \boldsymbol{\sigma} \cdot (\Delta \times \mathbf{E} - \mathbf{E} \times \Delta) - \frac{c_4}{U_0^4} \frac{g}{2M_0} \boldsymbol{\sigma} \cdot \mathbf{B} \\ & + c_5 \frac{a^2 \Delta^{(4)}}{24M_0} - c_6 \frac{a(\Delta^{(2)})^2}{16nM_0^2} + O(v^6) \end{aligned}$$

The stability parameter n is algorithmic, not physical; we use $n = 4$.

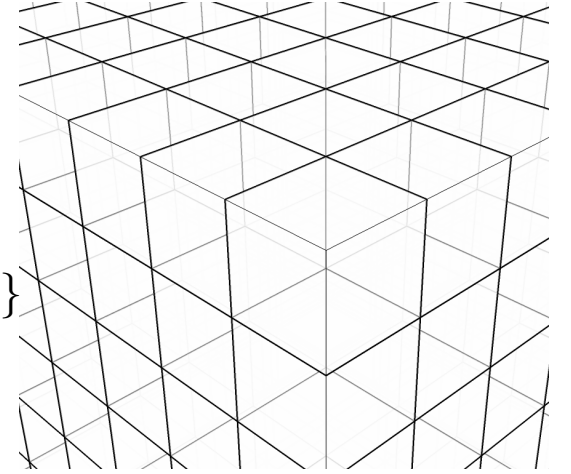
Tadpole improvement via average link in Landau gauge: $U_0 = 0.8463$.

We use tadpole-improved leading order: $c_i = 1$ for all i .

The bottom quark bare mass $M_0 = 1.95$ is set by fitting the experimental $\Upsilon(1S)$ mass.

Creation operators for “ground states”

Λ^{PC}	J^{PC}	$^{2S+1}L_J$	Ω
A_1^{-+}	0^{-+}	1S_0	1
T_1^{--}	1^{--}	3S_1	$\{\sigma_1, \sigma_2, \sigma_3\}$
T_1^{+-}	1^{+-}	1P_1	$\{\Delta_1, \Delta_2, \Delta_3\}$
A_1^{++}	0^{++}	3P_0	$\Delta_1\sigma_1 + \Delta_2\sigma_2 + \Delta_3\sigma_3$
T_1^{++}	1^{++}	3P_1	$\{\Delta_2\sigma_3 - \Delta_3\sigma_2, \Delta_3\sigma_1 - \Delta_1\sigma_3, \Delta_1\sigma_2 - \Delta_2\sigma_1\}$
E^{++}	2^{++}	3P_2	$\{(\Delta_1\sigma_1 - \Delta_2\sigma_2)/\sqrt{2}, (\Delta_1\sigma_1 + \Delta_2\sigma_2 - 2\Delta_3\sigma_3)/\sqrt{6}\}$
T_2^{++}	2^{++}	3P_2	$\{\Delta_2\sigma_3 + \Delta_3\sigma_2, \Delta_3\sigma_1 + \Delta_1\sigma_3, \Delta_1\sigma_2 + \Delta_2\sigma_1\}$
E^{-+}	2^{-+}	1D_2	$\{(D_{11} - D_{22})/\sqrt{2}, (D_{11} + D_{22} - 2D_{33})/\sqrt{6}\}$
T_2^{-+}	2^{-+}	1D_2	$\{D_{23}, D_{31}, D_{12}\}$
E^{--}	2^{--}	3D_2	$\{(D_{23}\sigma_1 - D_{13}\sigma_2)/\sqrt{2}, (D_{23}\sigma_1 + D_{31}\sigma_2 - 2D_{12}\sigma_3)/\sqrt{6}\}$
T_2^{--}	2^{--}	3D_2	$\{(D_{22} - D_{33})\sigma_1 + D_{13}\sigma_3 - D_{12}\sigma_2, (D_{33} - D_{11})\sigma_2 + D_{21}\sigma_1 - D_{23}\sigma_3, (D_{11} - D_{22})\sigma_3 + D_{32}\sigma_2 - D_{31}\sigma_1\}$
A_2^{--}	3^{--}	3D_3	$D_{12}\sigma_3 + D_{23}\sigma_1 + D_{31}\sigma_2$
A_2^{+-}	3^{+-}	1F_3	D_{123}
T_2^{+-}	3^{+-}	1F_3	$\{D_{122} - D_{133}, D_{233} - D_{211}, D_{311} - D_{322}\}$
A_2^{++}	3^{++}	3F_3	$(D_{221} - D_{331})\sigma_1 + (D_{332} - D_{112})\sigma_2 + (D_{113} - D_{223})\sigma_3$
T_1^{-+}	4^{-+}	1G_4	$\{D_{2223} - D_{3332}, D_{3331} - D_{1113}, D_{1112} - D_{2221}\}$
A_1^{--}	4^{--}	3G_4	$(D_{2223} - D_{3332})\sigma_1 + (D_{3331} - D_{1113})\sigma_2 + (D_{1112} - D_{2221})\sigma_3$
E^{+-}	5^{+-}	1H_5	$\{(D_{23111} - D_{13222})/\sqrt{2}, (D_{23111} + D_{13222} - 2D_{12333})/\sqrt{6}\}$
A_2^{-+}	6^{-+}	1I_6	$D_{112222} + D_{223333} + D_{331111} - D_{221111} - D_{332222} - D_{113333}$
A_1^{+-}	9^{+-}	1L_9	$D_{12223333} + D_{23331111} + D_{31112222} - D_{13332222} - D_{21113333} - D_{32221111}$



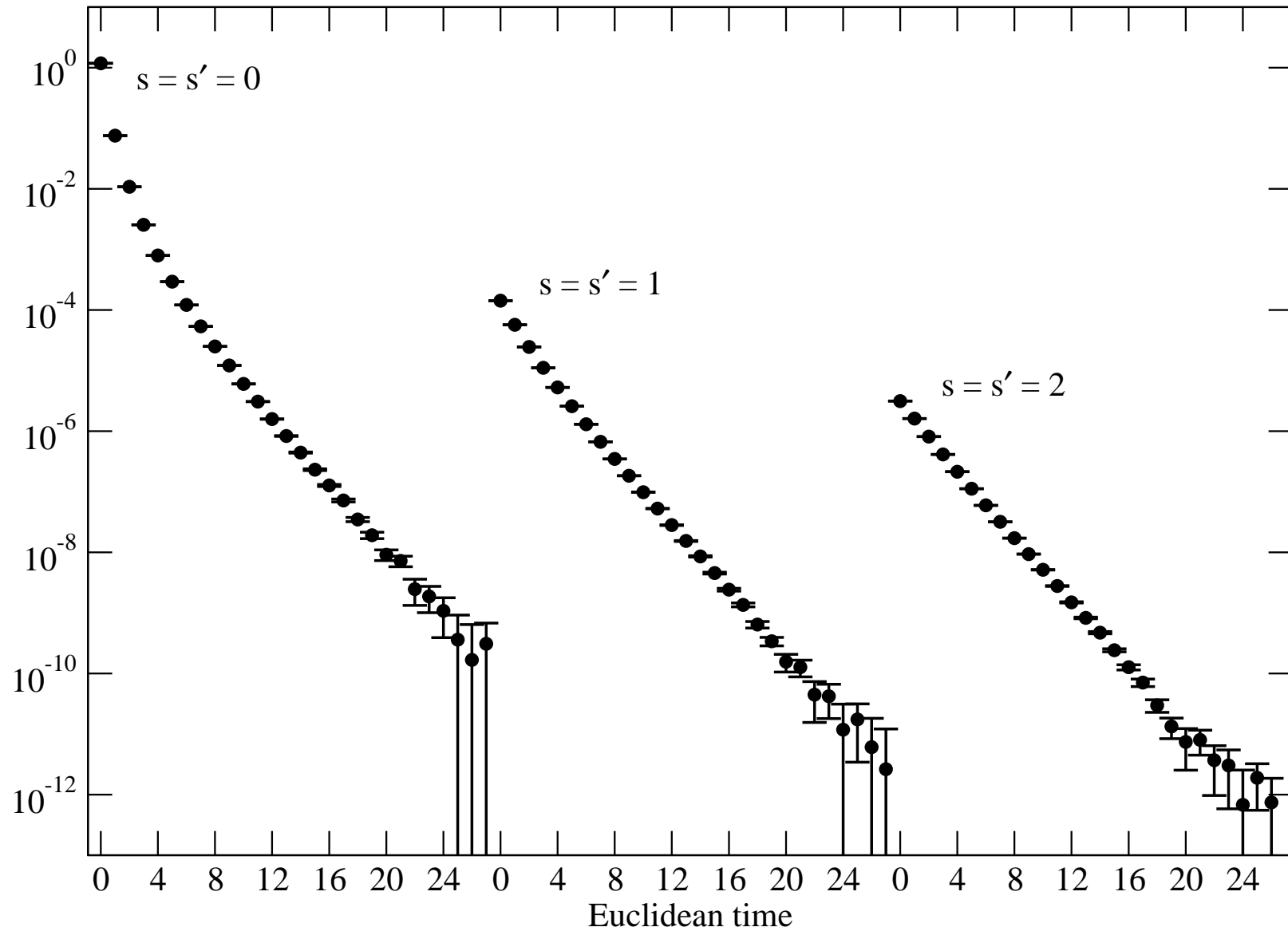
Simulation details

- 64 random-U(1) wall sources per configuration
- gauge-invariant smearing: $\psi(x) \rightarrow (1 + 0.15\Delta^2)^{8s} \psi(x)$ with $s = 0, 1, 2$
- stout links (Morningstar&Peardon,2004) for F-wave and G-wave operators
- a generalized multi-exponential fit:

$$g(t - t_0) = \sum_{n=1}^{N'} \sum_{s=0}^2 \sum_{s'=0}^2 f_s(n) f_{s'}(n) e^{-E_n(t-t_0)} + \sum_{n=N'+1}^N \sum_{s=0}^2 \sum_{s'=0}^2 f_{s,s'}(n) e^{-E_n(t-t_0)}$$

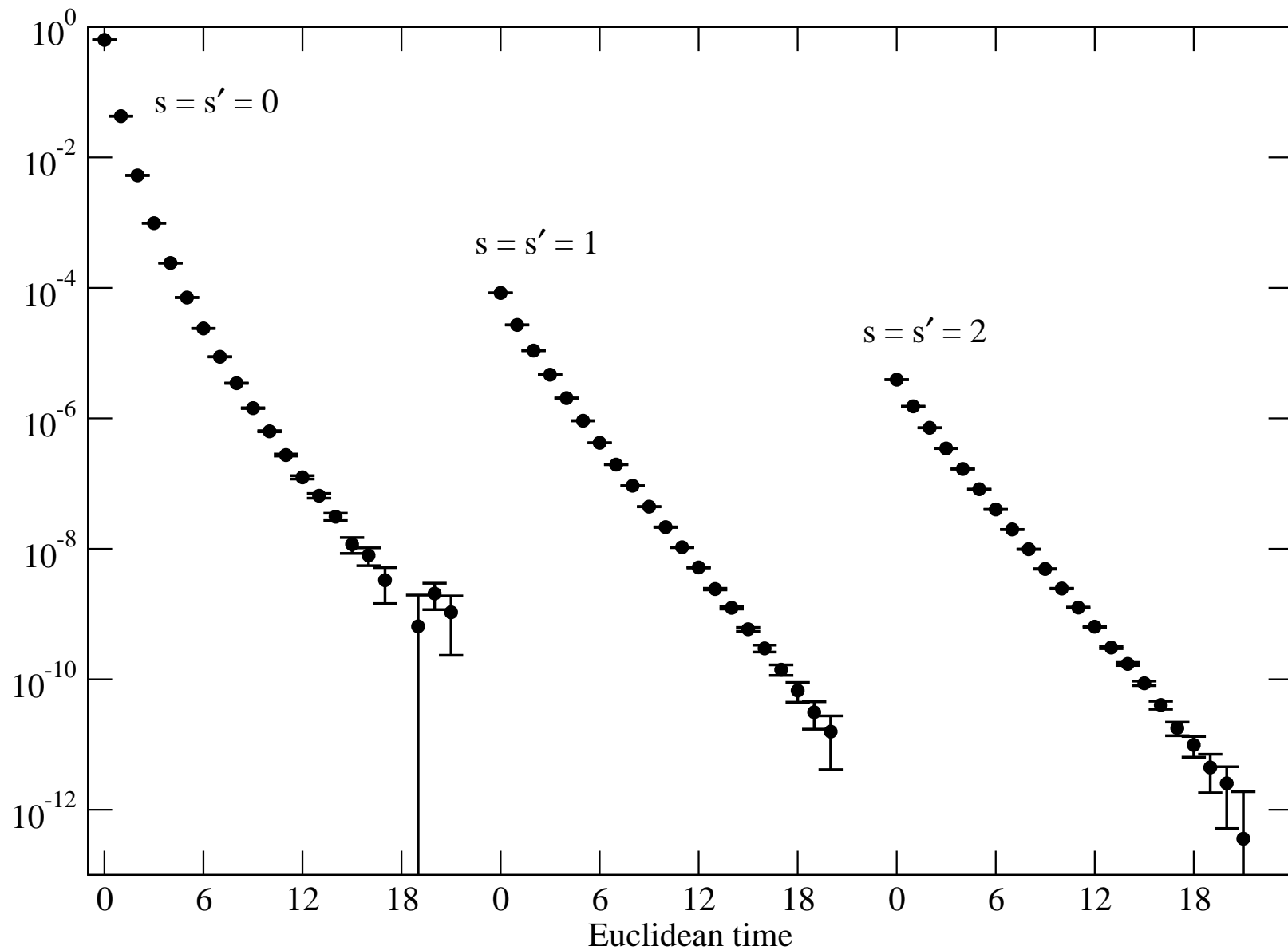
Sample E^{--} correlation functions.

(The lightest meson is 3D_2 .)



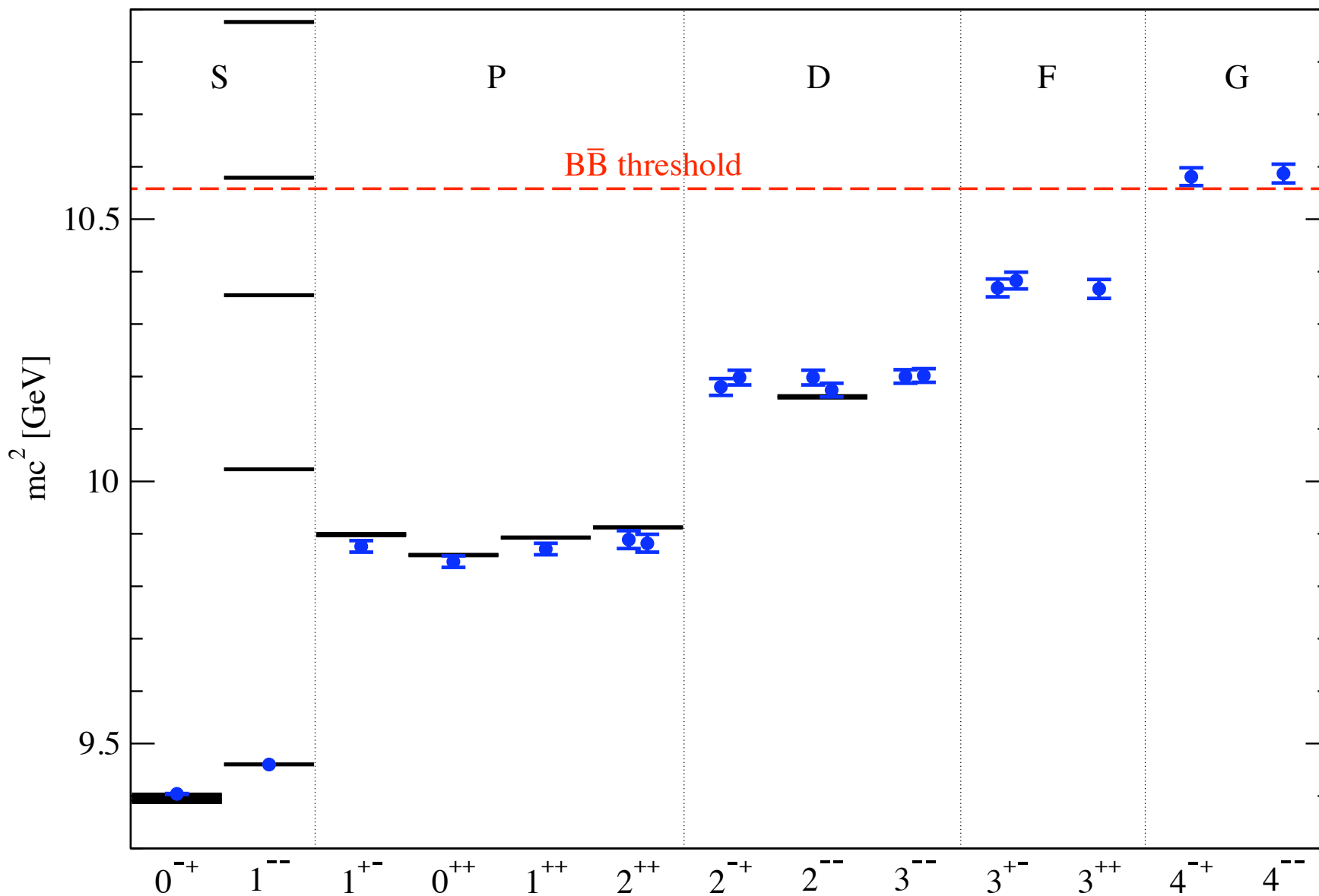
Sample T_2^{+-} correlation functions.

(The lightest meson is 1F_3 .)



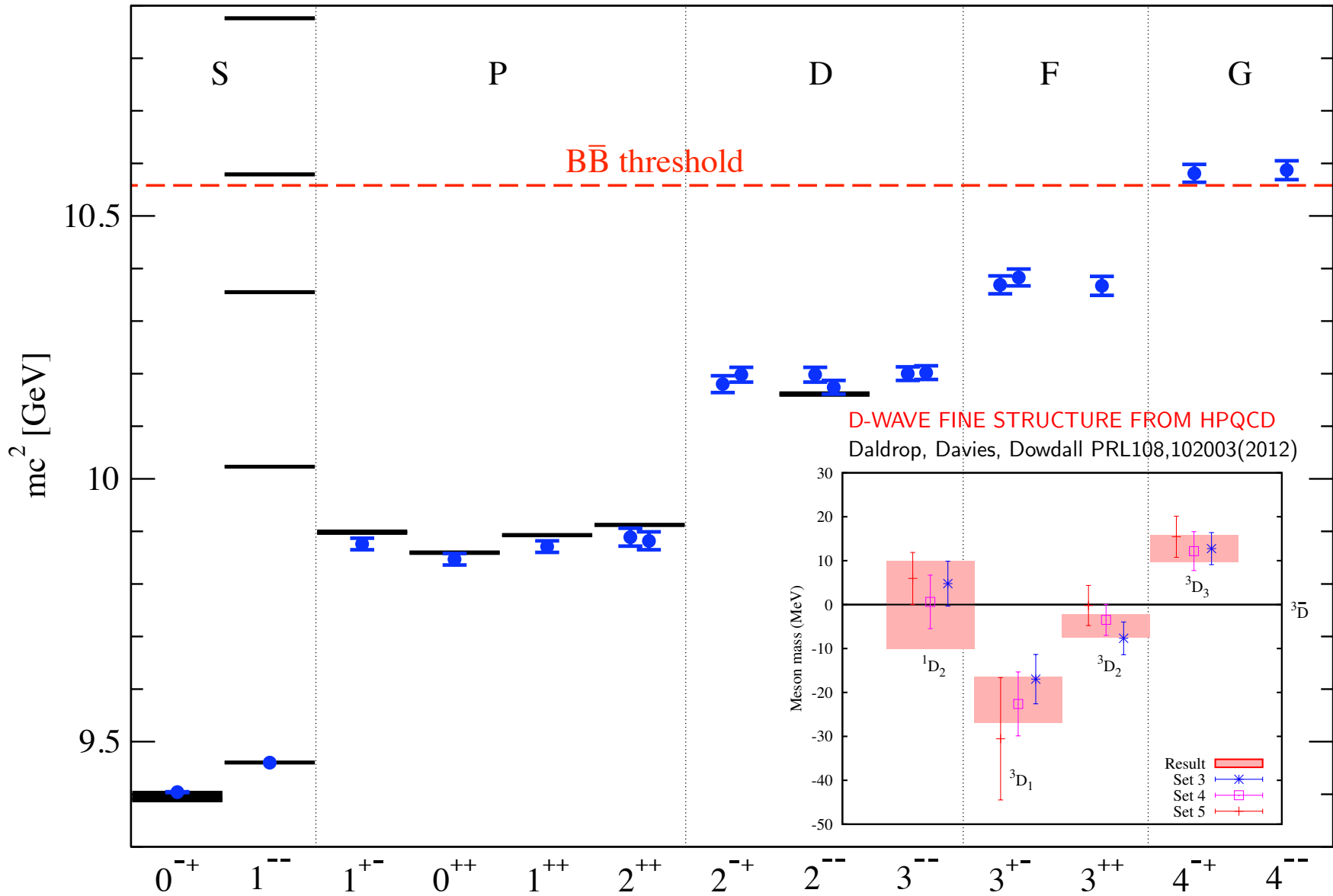
“ground state” bottomonium spectrum

Lattice (with statistical errors) and experiment.

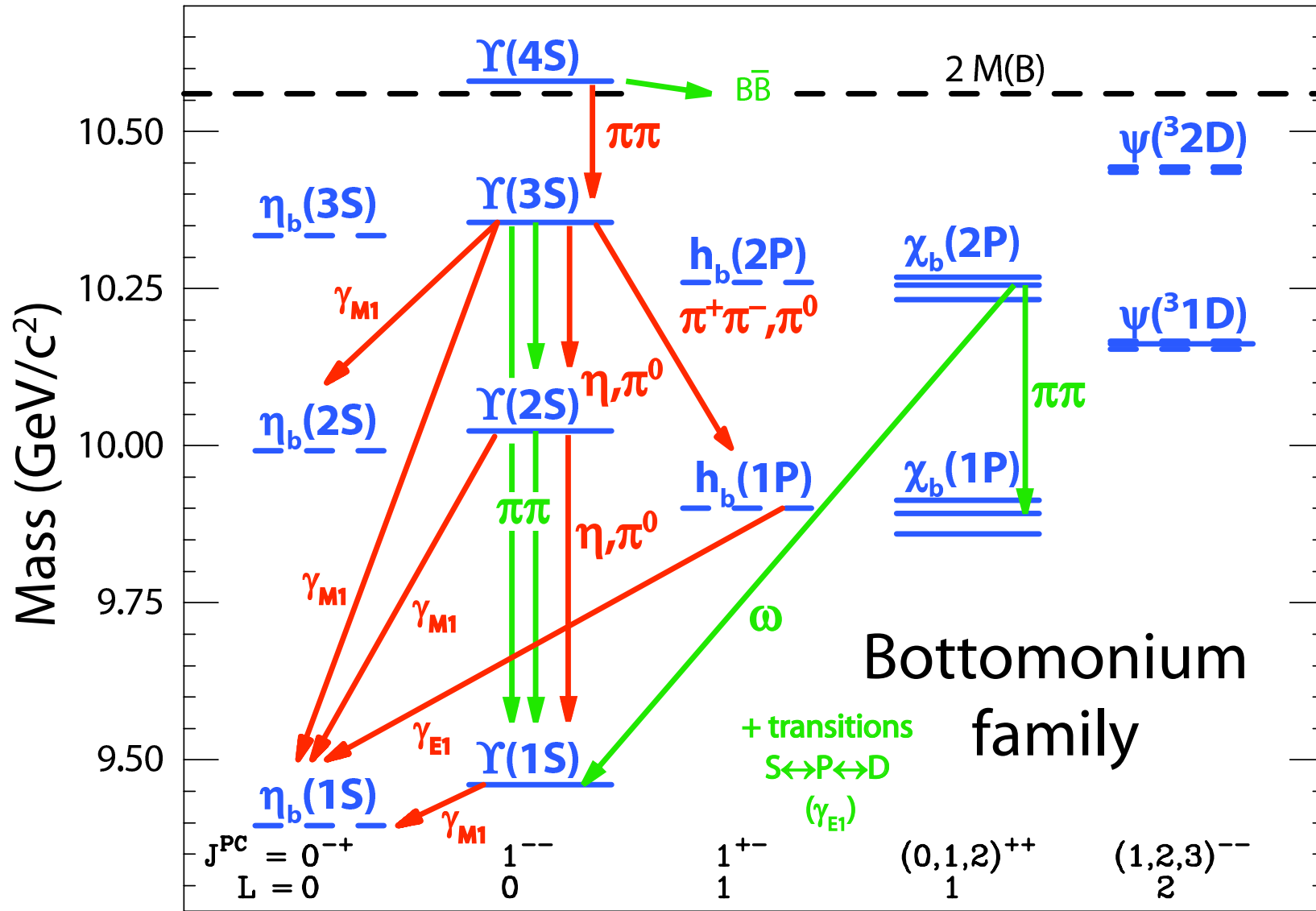


"ground state" bottomonium spectrum

Lattice (with statistical errors) and experiment.

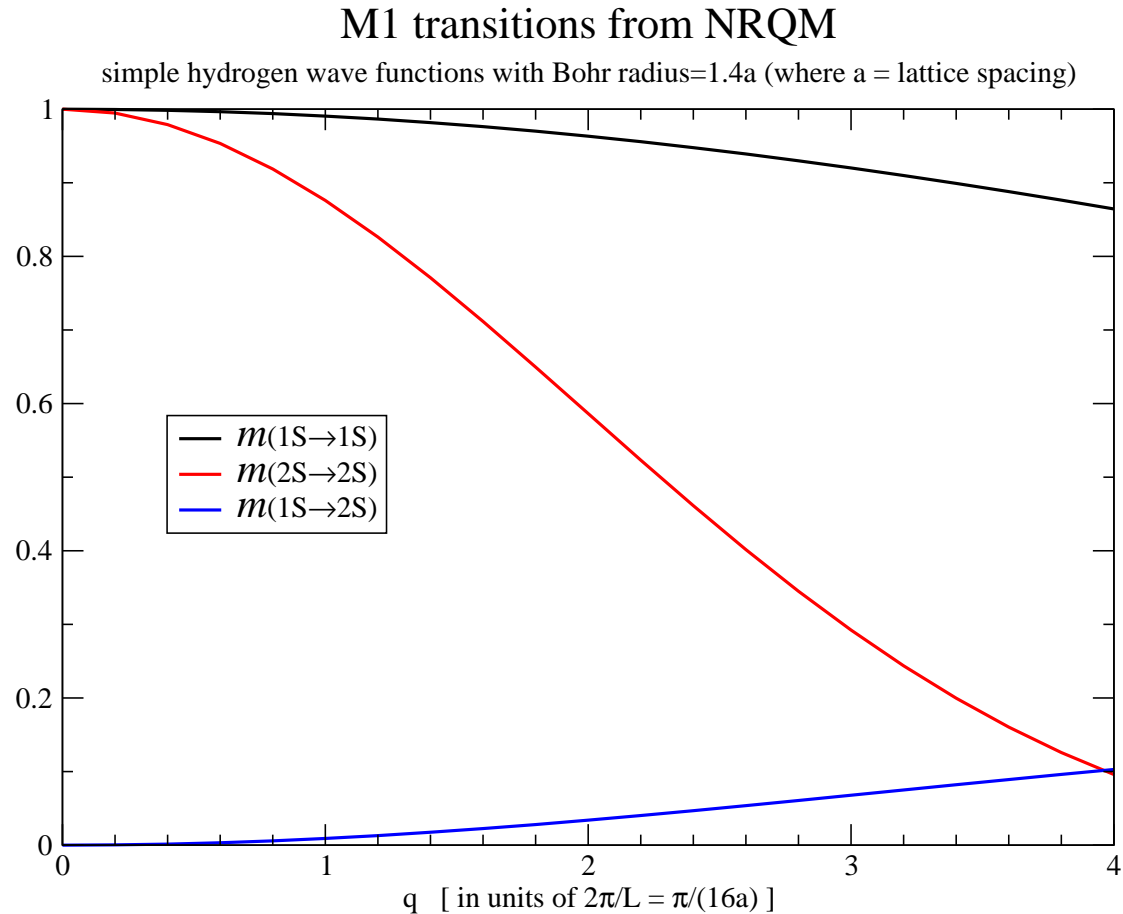


Radiative transitions in bottomonium



Pseudoscalar \leftrightarrow vector M1 transitions in the nonrelativistic quark model require

$$\mathcal{M}(nS \rightarrow n'S) = \int_0^\infty R_{n'}(r)R_n(r)j_0(qr/2)r^2dr$$



Therefore **hindered transitions** are subtle: recoil, spin, relativistic, ...

Spin terms in the Hamiltonian

$$\delta H^{(4)} = -\frac{c_4}{U_0^4} \frac{g}{2M_0} \boldsymbol{\sigma} \cdot \mathbf{B} - \frac{c_3}{U_0^4} \frac{g}{8M_0^2} \boldsymbol{\sigma} \cdot (\Delta \times \mathbf{E} - \mathbf{E} \times \Delta)$$

$$\delta H^{(6)} = -\frac{c_7}{U_0^4} \frac{g}{8M_0^3} \{\Delta^{(2)}, \boldsymbol{\sigma} \cdot \mathbf{B}\} - \frac{c_8}{U_0^4} \frac{3g}{64M_0^4} \{\Delta^{(2)}, \boldsymbol{\sigma} \cdot (\Delta \times \mathbf{E} - \mathbf{E} \times \Delta)\}$$

Transition operators

$$\mathcal{O}_{\text{magnetic}}^{(4)} = \sum_{\mathbf{x}} \sigma_3 e^{i\mathbf{k} \cdot \mathbf{x}}$$

$$\mathcal{O}_{\text{electric}}^{(4)} = \frac{1}{4M_0} \sum_{\mathbf{x}} i\sigma_3 \Delta_{1k}$$

$$\mathcal{O}_{\text{magnetic}}^{(6)} = \frac{1}{4M_0^2} \sum_{\mathbf{x}} \{\Delta^{(2)}, \sigma_3 e^{i\mathbf{k} \cdot \mathbf{x}}\}$$

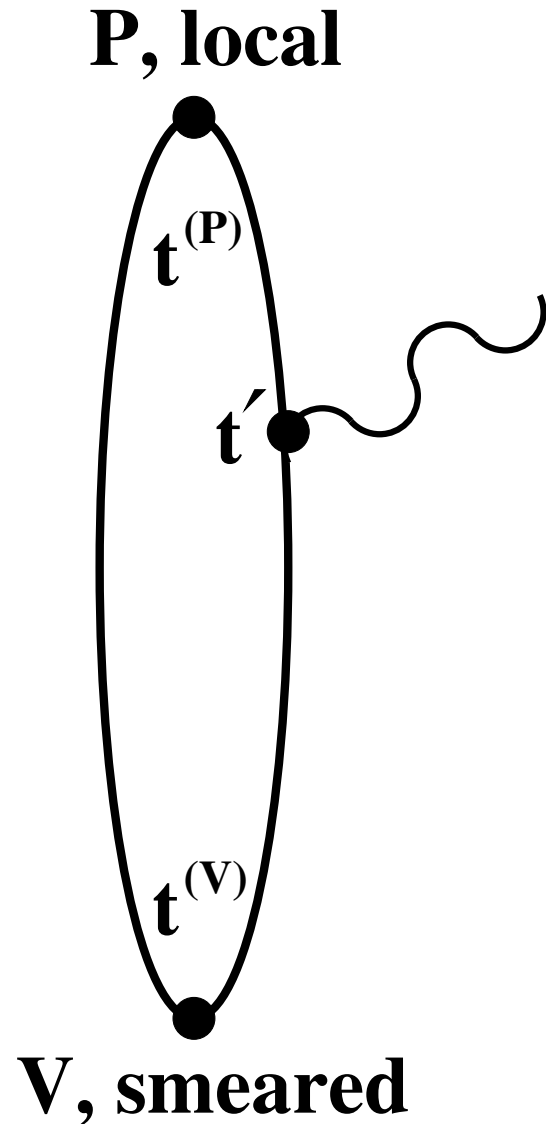
$$\mathcal{O}_{\text{electric}}^{(6)} = \frac{3}{32M_0^2} \sum_{\mathbf{x}} \{\Delta^{(2)}, i\sigma_3 \Delta_{1k}\}$$

Three-point functions

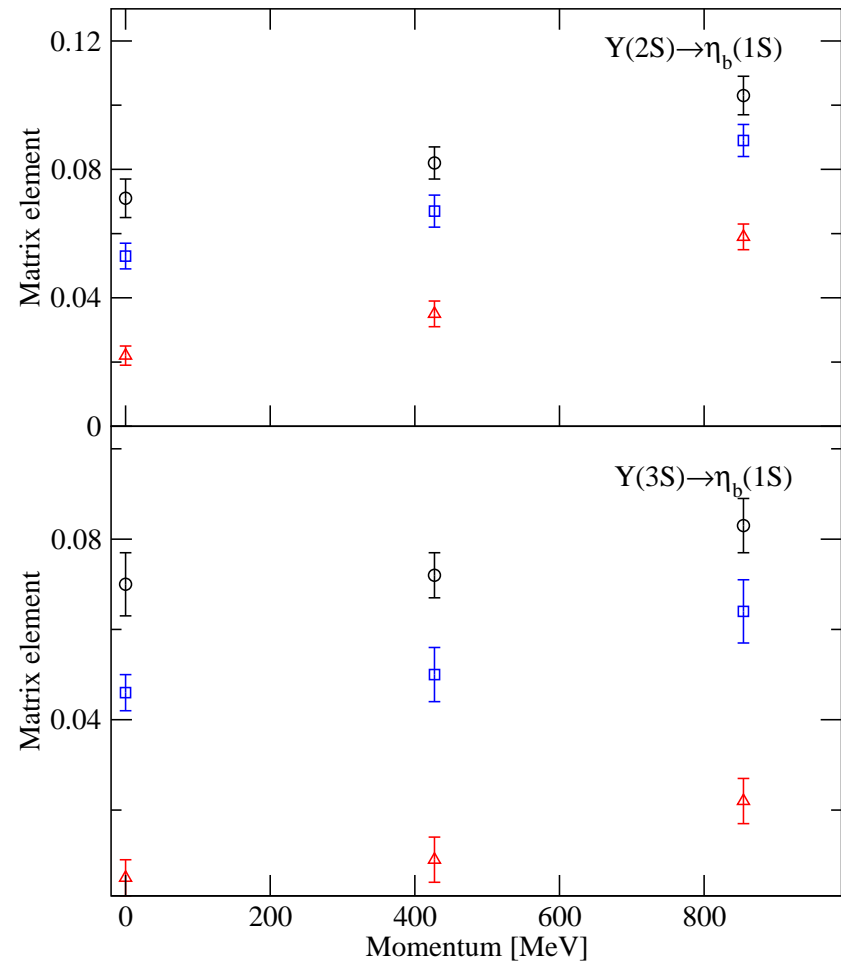
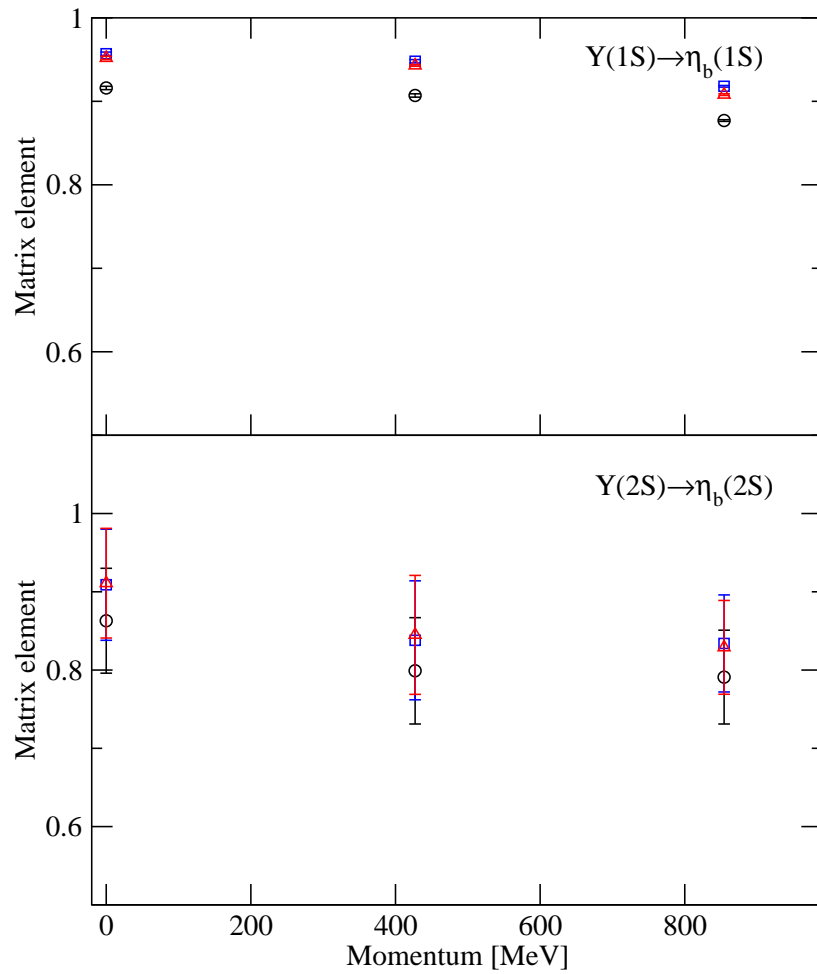
$$\sum_n \sum_{n'} c_s^{(V)}(n) A_{nn'}^{(VP)} c_t^{(P)}(n') \exp\left(-E_n^{(V)}(t' - t^{(V)})\right) \exp\left(-E_{n'}^{(P)}(t^{(P)} - t')\right)$$

We use $nn' = 11, 12, 21, 13, 31, 22$.

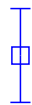
The time fit range is $t^{(P)} + 2 < t' < t^{(V)} - 2$.



Transition matrix elements



$\delta H^{(4)}$ with $O_{\text{magnetic}}^{(4)}$

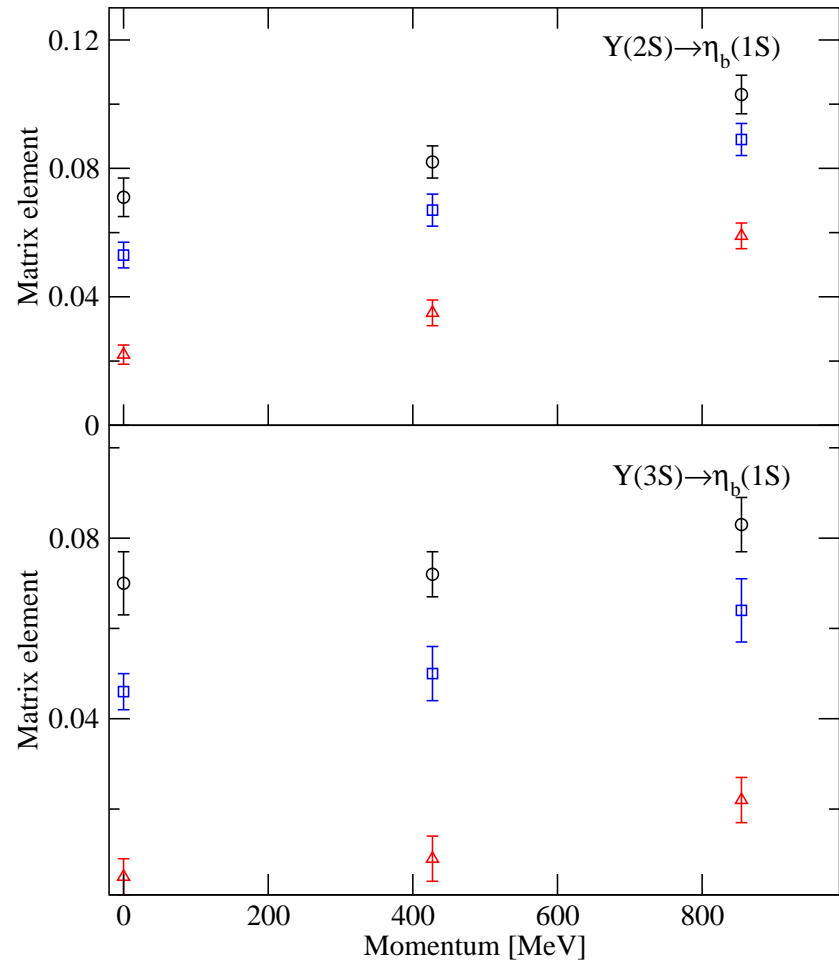
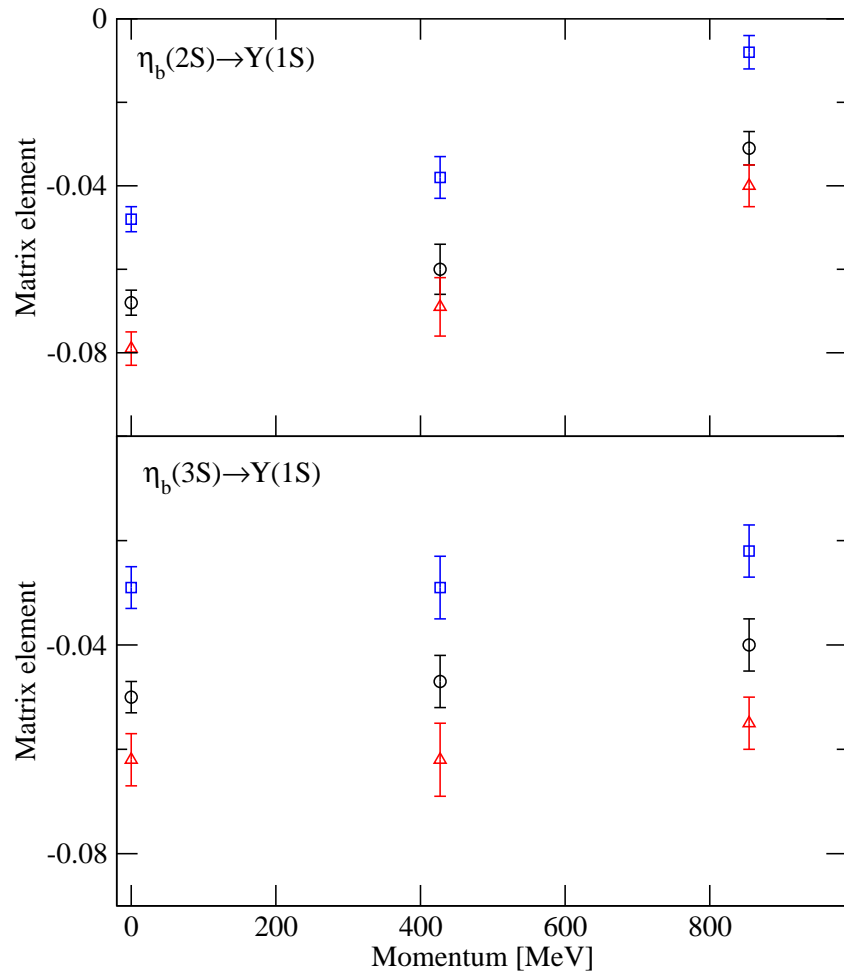


$\delta H^{(4)} + \delta H^{(6)}$ with $O_{\text{magnetic}}^{(4)}$

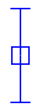


$\delta H^{(4)} + \delta H^{(6)}$ with $O_{\text{magnetic}}^{(4)} + O_{\text{magnetic}}^{(6)}$

Transition matrix elements



$\delta H^{(4)}$ with $O_{\text{magnetic}}^{(4)}$

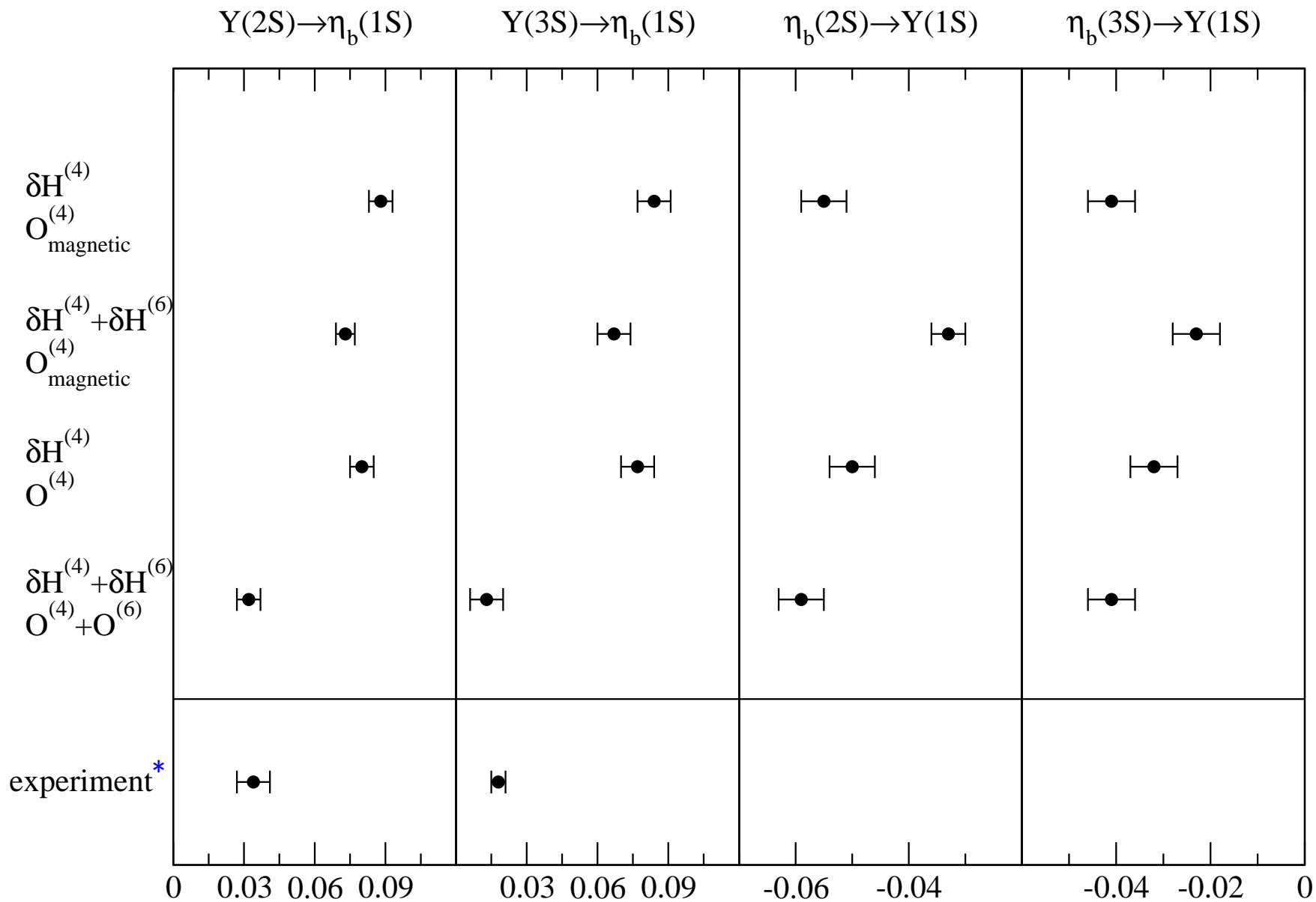


$\delta H^{(4)} + \delta H^{(6)}$ with $O_{\text{magnetic}}^{(4)}$



$\delta H^{(4)} + \delta H^{(6)}$ with $O_{\text{magnetic}}^{(4)} + O_{\text{magnetic}}^{(6)}$

Transition matrix elements at physical momentum



*BABAR Collaboration, PRL 101, 071801 (2008) and PRL 103, 161801 (2009).

Conclusions

bottomonium masses:

- Operators for all 16 lattice “ground states” have been constructed.
- S, P, D, F and G waves are observed.

M1 transitions:

- Sensitivity to small effects \Rightarrow a valuable challenge for lattice simulations.
- Relativistic corrections are large.
- $\Upsilon(2S) \rightarrow \eta_b(1S)$ and $\Upsilon(3S) \rightarrow \eta_b(1S)$ agree with experiment.
- $\eta_b(2S) \rightarrow \Upsilon(1S)$ and $\eta_b(3S) \rightarrow \Upsilon(1S)$ are predicted. **◀ Experiments would provide a stringent test!**